

Examining runner's outdoor heat exposure using urban microclimate modeling and GPS trajectory mining



Xiaojiang Li^{a,*}, Guoqing Wang^{b,c}

^a Department of Geography and Urban Studies, Temple University, Philadelphia, PA 19038, United States of America

^b NASA Goddard Space Flight Center, Greenbelt, MD, 20771, USA

^c Science Systems and Applications, Inc. (SSAI), Lanham, MD, 20706, USA

ARTICLE INFO

Keywords:

Personal heat exposure
Urban heat
GPS trajectories
Urban climate modeling
Mean radiant temperature (T_{mrt})

ABSTRACT

It is important to quantify human heat exposure in order to evaluate and mitigate the negative impacts of heat on human well-being in the context of global warming. This study proposed a human-centric framework to examine human personal heat exposure based on anonymous GPS trajectories data mining and urban microclimate modeling. The mean radiant temperature (T_{mrt}) that represents human body's energy balance was used to indicate human heat exposure. The meteorological data and high-resolution 3D urban model generated from multispectral remotely sensed images and LiDAR data were used as inputs in urban microclimate modeling to map the spatio-temporal distribution of the T_{mrt} in the Boston metropolitan area. The anonymous human GPS trajectory data collected from fitness Apps was used to map the spatio-temporal distribution of human outdoor activities. By overlaying the anonymous GPS trajectories on the generated spatio-temporal maps of T_{mrt} , this study further examined the heat exposure of runners in different age-gender groups in the Boston area. Results show that there is no significant difference in terms of heat exposure for female and male runners. The female runners in the age of 45–54 are exposed to more heat than female runners of 18–24 and 25–34, while there is no significant difference among male runners. This study proposed a novel method to estimate human heat exposure, which would shed new light on mitigating the negative impacts of heat on human health.

1. Introduction

Extreme heat has become one of the most serious human health threats to urban residents in the context of global climate change and the urban heat island effect (Li & Ratti, 2019; Reidmiller et al., 2018; Stone, Hess, & Frumkin, 2010; Venter, Krog, & Barton, 2020). One-fifth of hazard deaths are caused by extreme heat events in the United States (Borden & Cutter, 2008). The number of deaths caused by extreme heat is almost as large as the deaths caused by flooding and hurricanes combined (National Weather Service, 2018). Too much heat exposure can cause human body's energy imbalance and increase human body temperature beyond a safe temperature, which would further impact human thermal comfort, physical and mental health, and cognitive performance (Hajat, O'Connor, & Kosatsky, 2010; Kuras et al., 2017; Parsons, 2003; Zhang, de Dear, & Hancock, 2019). Elderly people and people with pre-existing cardiovascular and respiratory diseases tend to be more vulnerable to the intense heat exposure (Hajat et al., 2010; Kovats & Hajat, 2008). Studying how humans are exposed to heat is thus

important for mitigating the negative impacts of heat exposure on human health and building resilience to more and more frequent and intensive heat events.

Traditionally, the ambient temperature from fixed-site weather stations is usually used to represent the intensity of heat events (Gasparri et al., 2015; Ho & Wong, 2019; Noelke et al., 2016; Wang et al., 2018). However, the ambient temperature cannot fully indicate human personal heat exposure without considering the human travel patterns and the indoor and outdoor environment (Kuras et al., 2017; Milà et al., 2020). In addition, the ambient temperature measured at those sparsely distributed weather stations cannot represent the spatial variations of urban heat. With the virtue of large and seamless coverage, the land surface temperature derived from satellite-based thermal imageries was also widely used to indicate the distribution of heat and investigate the impacts of heat on human well-being (Harlan, Declet-Barreto, Stefanov, & Petitti, 2013; Jenerette et al., 2016; Pearsall, 2017; Wang, Li, Myint, Zhao, & Wentz, 2019). However, the land surface temperature derived from remotely sensed data represents the temperature of the tops of tree

* Corresponding author.

E-mail address: lixiaojiang.gis@gmail.com (X. Li).

canopies, building roofs, and the ground surface, which cannot fully indicate the actual heat that humans exposed on the ground (Li & Ratti, 2019). The land surface temperature derived from thermal imageries that are captured at certain points in time cannot represent those spatially and temporally varying factors that impact human heat stress, such as, air temperature, humidity, shade, wind, etc. The land surface temperature has also been proved not to have strong associations with human health conditions (Stone Jr, Lanza, Mallen, Vargo, & Russell, 2019). In addition, it would be difficult to estimate human personal heat exposure without considering human travel patterns.

Using wearable sensors to measure human heat exposure is a promising method to measure personal heat exposure in real-time (Milà et al., 2020; Muller et al., 2015). Individuals going about their daily lives using small and portable sensors is a relatively objective way to measure more personalized heat exposure (Bailey et al., 2020; Basu & Samet, 2002; Bernhard et al., 2015; Hass & Ellis, 2019; Milà et al., 2020). However, the accuracy of the wearable sensor-based method is sensitive to the placement of the sensors and the continuous repositioning of the sensors while users moving would also impact the measured results (Kuras et al., 2017). In addition, the sensor-based method is only able to measure the heat exposure for those people with sensors, which limits the sensor-based method to a small sample population and a small geographical area.

The model simulation-based method provides an indirect way to estimate personal heat exposure at a large scale (Gasparetto & Nesselser, 2020; Honjo et al., 2018; Li & Ratti, 2019; Middel, Lukasczyk, & Maciejewski, 2017; Vanos et al., 2019). Gasparetto and Nesselser (2020) used historical weather data to calculate the marathon runner's heat exposure index and evaluated the impact of the thermal environment on the performance of runners in New York City. However, the calculated heat exposure index doesn't consider the spatial variations of heat exposure, which are significantly different street by street because of the shadow and other microclimate factors caused by urban structures. Honjo et al. (2018) modeled and evaluated the thermal comfort along the Tokyo Olympic marathons course, which would aid in taking actions for mitigating the heat stress. Middel et al. (2017) used RayMan model to generate thermal comfort maps and implemented an optimized routing to maximize pedestrian's thermal comfort. Li and Ratti (2019) estimated the spatio-temporal distribution of sun exposure using the hemispherical images generated from the Google Street View images to simulate the solar radiation at the street canyon levels. Although the method shows the potentials to estimate human sunlight exposure, however, the method is focused on the spatio-temporal distribution of sunlight exposure within street canyons, and personal level heat exposure was not considered.

This study proposed a framework to estimate human personal heat exposure by combining urban microclimate modeling and human travel patterns that are in form of GPS trajectories at a fine level. The anonymous trajectories of anonymous fitness app users in the Boston area were used to indicate human travel patterns. The fine-level LiDAR data, building footprint map, and multispectral remotely sensed imageries were used to build the urban three-dimensional model and simulate the solar radiation fluxes in street canyons at the same time of those trajectories. This study mapped the spatio-temporal distributions of mean radiant temperature (T_{mrt}), which is an objective indicator of the human body's energy balance with consideration of the solar and terrestrial radiation and meteorological data based on urban microclimate modeling. By overlaying the anonymous runner's GPS trajectories on the spatio-temporal distributions of T_{mrt} , this study calculated the human personal heat exposure level for anonymous runners and examined the different heat exposures among different age-gender groups of runners.

2. Study area and datasets

The study area is located in the Boston metropolitan area (Fig. 1), which majorly includes the city of Boston, Cambridge, and nearby

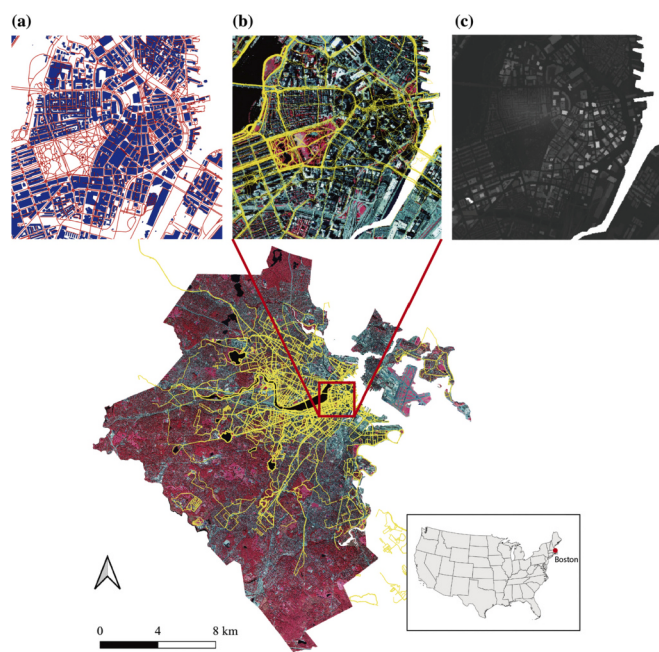


Fig. 1. The location of the study area and the datasets used in this study, (a) the open street map and the building footprint map, (b) the GPS trajectories and the multispectral NAIP imageries, (c) the generated digital surface model from LiDAR data.

towns. The Boston area has a humid continental climate that features cool summers and cold winters. July and early August are usually the hottest months of one year with an average temperature of 23 °C.

The datasets used in this study include anonymous runner's GPS trajectories, meteorological data, Light Detection and Ranging (LiDAR) cloud point data, multispectral satellite imageries, and building footprint map. The GPS trajectory data were collected from a popular fitness App during 2014–2015. The trajectory data includes GPS locations, trajectory mode (running, cycling, and walking), and age-gender information of anonymous users. The meteorological data that includes the weather condition, air temperature, direct and diffuse radiation, wind speed, and humidity, were collected from the National Renewable Energy Laboratory database (<https://maps.nrel.gov/nsrdb-viewer/>). The LiDAR data was collected from NOAA Digital coast datasets (<https://coast.noaa.gov/dataviewer/#/>) and used to generate the digital surface model (DSM) and the digital terrain model (DEM) using the spatial resolution of 1 m. The National Agriculture Imagery Program (NAIP) satellite imageries with a spatial resolution of 0.6 m and four bands (red, green, blue, and near-infrared) were used to generate the vegetation cover of the study area. The building footprint map was collected from the Microsoft building footprint database (<https://github.com/microsoft/USBuildingFootprints>). Fig. 1 shows the location of the study area and the collected datasets in the study area.

3. Methodology

3.1. Building height model and tree canopy height model generation

A high resolution three-dimensional urban model is required for modeling how solar radiation fluxes being obstructed and reaching the ground. The building height model and the tree canopy model are needed for modeling the obstructions of the building blocks and tree canopies on incoming solar radiation. In this study, the building height model was generated by overlaying the building footprint map (Fig. 1 (a)) on the digital surface model (DSM) (Fig. 1 (c)).

In order to generate the tree canopy height model, this study first generated the vegetation cover map from the NAIP multispectral

imagery using the thresholding method based on the NDVI (normalized difference vegetation index). Since the NDVI-based thresholding method cannot differentiate the tree canopies from grassland, therefore, this study further excluded those vegetation pixels with the height lower than 3 m based on the DSM to generate the tree canopy map. Validation results based on randomly selected samples show that the accuracy of the generated tree canopy cover map is as high as 95%, which makes it suitable for the following analyses. The tree canopy height model was then created by multiplying the binary tree canopy cover and the DSM.

3.2. Map-matching of GPS trajectories

The raw GPS trajectories are not aligned to streets well because of the noise and the block of GPS signal by obstructions in street canyons. Therefore, map-matching is needed to correct those trajectories to the corresponding streets (Li, Santi, Courtney, Verma, & Ratti, 2018; Malleson et al., 2018). In this study, the widely used Hidden Markov Chain method was implemented to do the map-matching (Newson & Krumm, 2009). The reference street map was firstly planarized into short street segments. The probabilities of each GPS coordinate point along one trajectory to nearby street segments are determined by the distances to nearby street segments and the probabilities are higher to closer street segments. The possibility of one GPS trajectory to a matching path is the multiplication of all the possibilities of all GPS trajectory points to connected street segments of the matching path. The optimal matched path of the GPS trajectory is the matching path that has the largest possibility. The Open Street Map (OSM) was used as the reference street map for the map-matching because the OSM covers complete streets and includes those small roads used by runners. Those highways and motorcycle ways, which are not accessible for pedestrians and runners, were excluded from the OSM in the map-matching. The map-matching results show that more than 85% of the trajectories can be matched successfully to the corresponding streets. Fig. 2 shows a comparison of several raw trajectories and the map-matched trajectories in the study area.



Fig. 2. The comparison of the four raw GPS trajectories (red) and the map-matched trajectories (green) in the study area. (For interpretation of the references to colour in this figure legend, the reader is referred to the web version of this article.)

3.3. Human heat exposure estimation

The mean radiant temperature (T_{mrt}) that indicates the human body's energy balance by considering the solar and terrestrial radiation, humidity is a standard method to indicate human thermal comfort (Ali-Toudert & Mayer, 2007; Mayer & Höpke, 1987). The T_{mrt} is strongly related to heat related mortalities (Thorsson et al., 2014). Therefore, in this study, the T_{mrt} was used to indicate human heat exposure. As one of the most accurate models that have been validated worldwide, the SOLWEIG model was used to calculate and map the spatio-temporal distributions of the T_{mrt} based on the building height model, tree canopy height model, and the meteorological data in the study area (Li, 2021; Lindberg & Grimmond, 2011; Lindberg, Holmer, & Thorsson, 2008; Lindberg, Holmer, Thorsson, & Rayner, 2014). Fig. 3 shows the process of T_{mrt} estimation based on the tree canopy height model, building height model, and meteorological data.

Based on the spatio-temporal distributions of the estimated T_{mrt} , the accumulated heat exposure for each trajectory can be estimated as,

$$HeatExpo = \int_{t_0}^{t_1} T_t(\text{lon}_t, \text{lat}_t, t) dt \quad (1)$$

where $HeatExpo$ is the accumulated heat exposure, t_0 is the starting time of a trajectory, t_1 is the ending time for the trajectory, T_t is the T_{mrt} at the time t and coordinate $(\text{lon}_t, \text{lat}_t)$. Because of the computational intensity to calculate T_{mrt} for the whole study area, therefore, this study estimated the T_{mrt} every 10 min from July 15th to August 15th, 2015 during sunny and clear weather, which are usually considered as the hottest days in one year, since the SOWEIG model is better to model human thermal comfort during the clear and hot season. Only those trajectories from July 15th to August 15th, 2015 in sunny and clear weather time windows were kept for the following analysis. Each trajectory was then split into different segments for the time windows of T_{mrt} maps and then overlaid on the T_{mrt} map of the same time (Fig. 3). Then the accumulated heat exposure ($^{\circ}\text{C}\cdot\text{min}$) would be,

$$HeatExpo = \sum_{i=0}^n d_i \cdot T_i \quad (2)$$

where n is the number of 10-min segments along one trajectory, the d_i is the duration of the runner staying in the i th segment, T_i is the average T_{mrt} along the i th segment for one trajectory. The SOWEIG is very time consuming for city-scale modeling, therefore, in this study, the input building height model and tree canopy height model were chopped into numbers of small tiles. The SOWEIG model was then run on those small tiles to calculate the T_{mrt} of different times on high performance computers and the results were then mosaiced to cover the whole study area.

This study further investigated the accumulated heat exposure differences for runners in different age-gender groups. The non-parametric Kruskal-Wallis one-way analysis of variance, which allows the comparison of more than two independent groups, was applied to determine the different heat exposure risks for runners in different age-gender groups.

4. Results

There are 3401 walking and running trajectories matched during the sunny and clear time from July 15th to August 15th, 2015. Fig. 4 (a) shows the spatial distribution of the number of runner's trajectories at the street level in the study area. It can be seen clearly that roads along the Charles River are the most popular for runners in the study area. Cambridge and the downtown of Boston are also popular places for runners. In addition, runners prefer to run along water bodies. Among the finally chosen 3401 anonymous trajectories, there are 1603 trajectories of female runners and 1798 trajectories of male runners. Fig. 4 (b) shows the distribution of the number of running trajectories for female

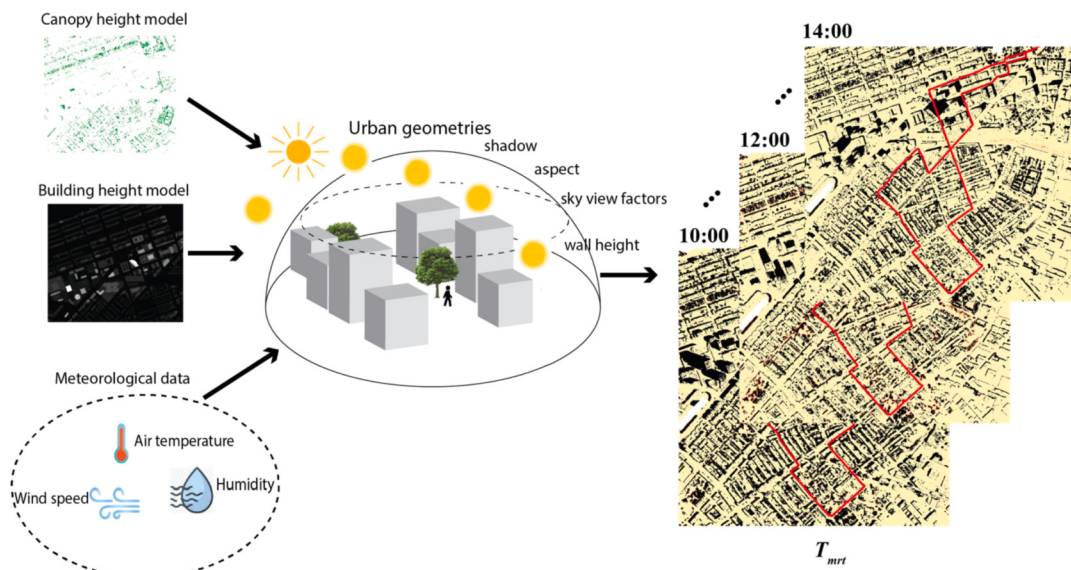


Fig. 3. Human heat exposure estimation based on GPS trajectory and the estimation of mean radiant temperature (T_{mrt}) using the SOLWEIG model based on building height model, canopy height model, and meteorological data.

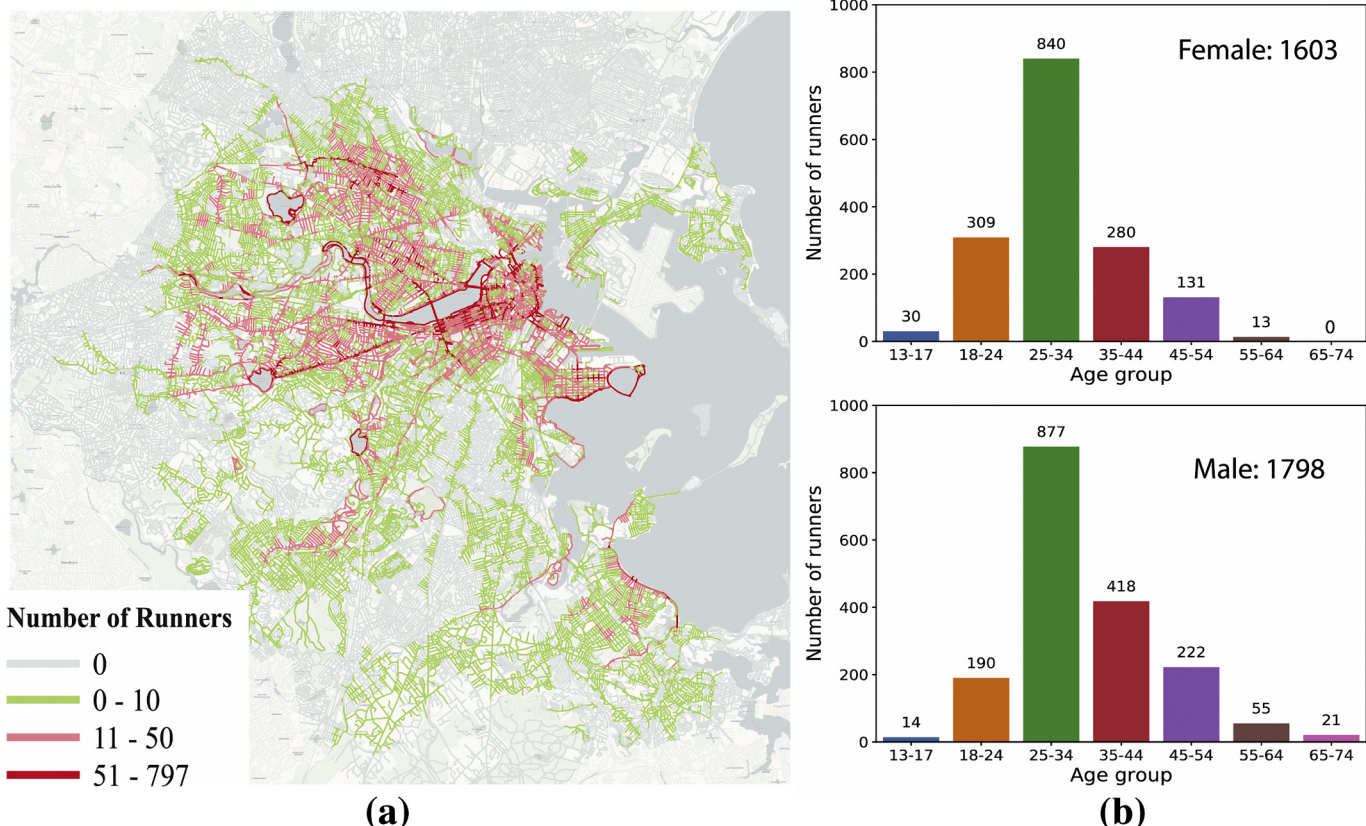


Fig. 4. The spatial distribution of the human fitness activities during sunny and clear time from July 15th to August 15th, 2015 in the Boston area, (a) the number of runners on each street, (b) the distribution of the numbers of runners in different age groups.

and male runners in different age-groups (Note: there is only one male runner in age 75–99 and not considered in the analysis). Most of the trajectories are from runners in the age of 25–34 for both female and male runners.

Fig. 5 shows the distribution of running duration and running distance of the running trajectories in the study area. It can be seen that most running trajectories last 20–40 min with distance of 1000 to 2000

m.

Fig. 6 shows the distributions of running distance and running duration in different age-gender groups from July 15th, 2015 to August 15th, 2015 in the study area. Generally, female runners in age-groups of 18–24 and 25–34 run longer distance and time than male runners in the same age-groups, while male runners in the age groups of 35–44 and 45–54 run longer distance and time than female runners of the same age

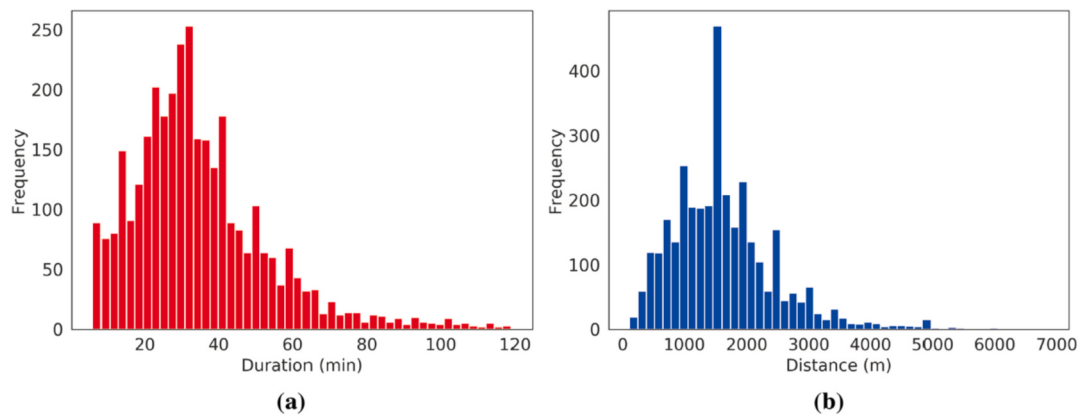


Fig. 5. The distribution of running time duration and running distance of anonymous trajectories in the study area, (a) the histogram of the running time duration, (b) the histogram of the running distance.

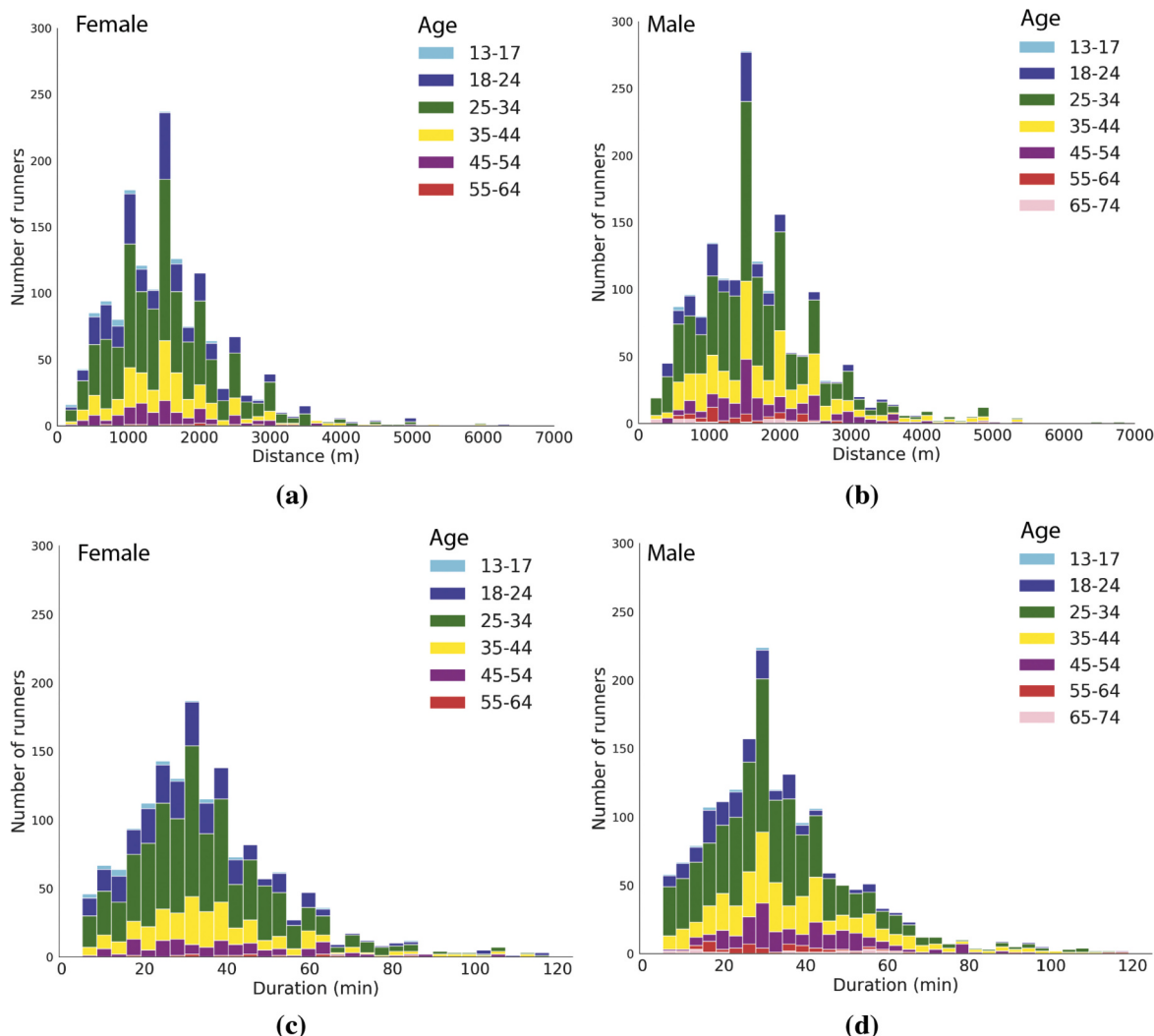


Fig. 6. The running distance and duration for different age-gender groups in the study area from July 15th to August 15th in 2015, (a) the distribution of running distance of female runners, (b) the distribution of the running distance of male runners, (c) the distribution of the running duration in minute of female runners, (d) the distribution of running duration in minute of male runners.

groups. The numbers of runners in other age groups are too small for the comparison (Fig. 6).

Fig. 7 (a) presents the spatial distribution of the T_{mrt} on a typical day of July 20th, 2015 at different times for a portion of the study area. The

T_{mrt} is influenced significantly by the shadow distributions cast by the buildings and tree canopies at different times. By overlaying the anonymous trajectories on the T_{mrt} of the same time in the study area, this study estimated the accumulated heat exposure for each trajectory.

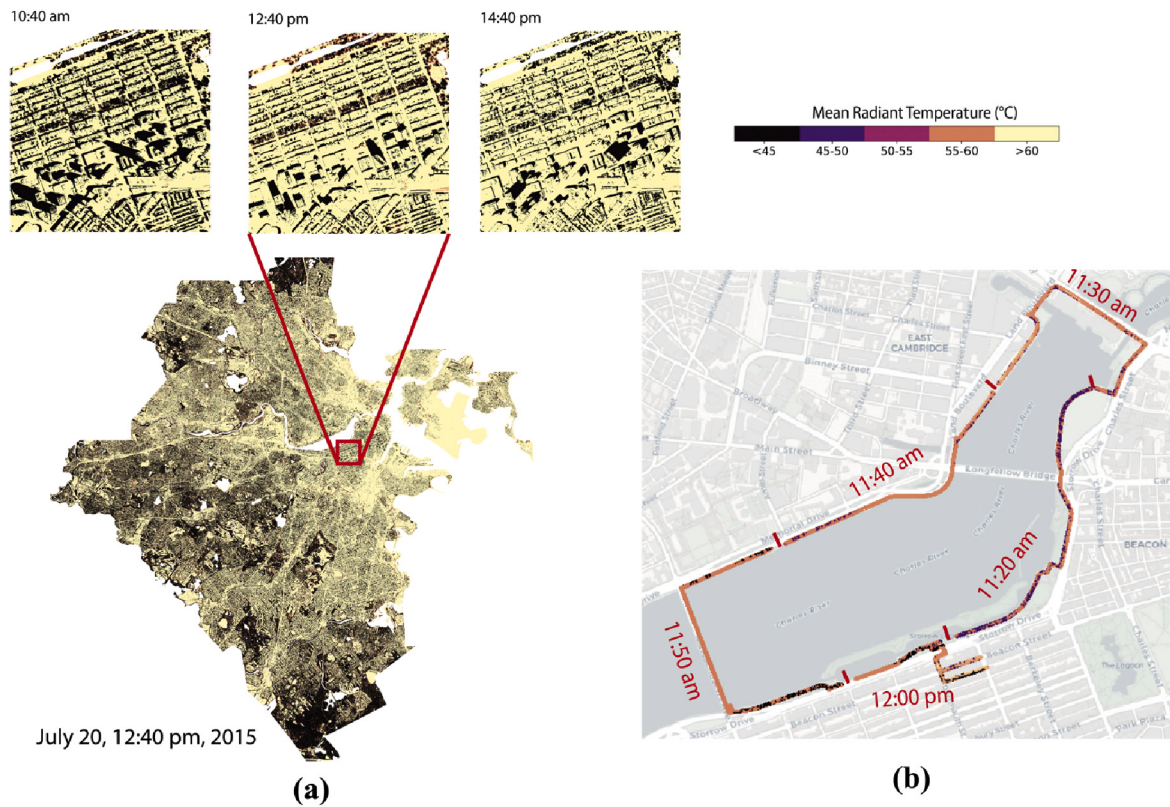


Fig. 7. The spatio-temporal distribution of the T_{mrt} and a runner's heat exposure, (a) the spatio-temporal distribution of the T_{mrt} on July 20th, 2015 at different time points, (b) the overlay of an anonymous trajectory on T_{mrt} maps for estimating the accumulated heat exposure.

Fig. 7 (b) shows the heat exposure along an anonymous trajectory on July 20th, 2015 in the study area.

For all the trajectories, descriptive analysis results show that the mean accumulated heat exposure is 1486.59 ($^{\circ}\text{C}\cdot\text{min}$) with the standard deviation of 921.23 ($^{\circ}\text{C}\cdot\text{min}$). **Fig. 8** shows the boxplot of the heat exposure for runners in different age groups in the study area. The

Kruskal-Wallis test shows that the heat exposure for runners in age 45–54 is significantly higher than runners in ages of 18–24 ($p < 0.05$) and 25–34 ($p < 0.05$). There is no significant difference in terms of heat exposure among other age groups.

Fig. 9 shows the histograms of the accumulated heat exposure for runners in different age-gender groups in the study area. It can be seen clearly that for both female and male runners, the accumulated heat exposure of most runners falls into the range of 1000 ($^{\circ}\text{C}\cdot\text{min}$) to 2000 ($^{\circ}\text{C}\cdot\text{min}$). **Fig. 10** shows the boxplots of the heat exposure for female and male runners in different age groups. For female runners, the heat exposure in the age group of 45–54 is significantly higher than runners in the age groups of 18–24 ($p < 0.05$) and 25–34 ($p < 0.05$) (**Fig. 10** (a)). There is no significant difference in terms of heat exposure among other age groups. For male runners, there is no significant difference in terms of heat exposure for runners in different age groups (**Fig. 10** (b)). Kruskal-Wallis test results show that for female and male runners of the same age groups, there is no significant difference in terms of heat exposure.

5. Discussion

Extreme heat increasingly becomes a major public health risk for urban residents especially in the context of global warming and urban heat island. Too much heat exposure would cause human body's energy imbalance, which further lead to heat-related morbidity and mortality ([Kuras et al., 2017](#); [Nazarian et al., 2021](#); [Parsons, 2003](#)). The heat exposure level of an individual is influenced by the surrounding thermal environment as well as the travel pattern of the individual. However, most of the widely used heat metrics are not human-centric and tend to focus on indicating the surrounding thermal environment. This study proposed a novel human-centric framework to estimate human outdoor heat exposure based on fine scale urban microclimate modeling and anonymous human GPS trajectories mining. The high-resolution

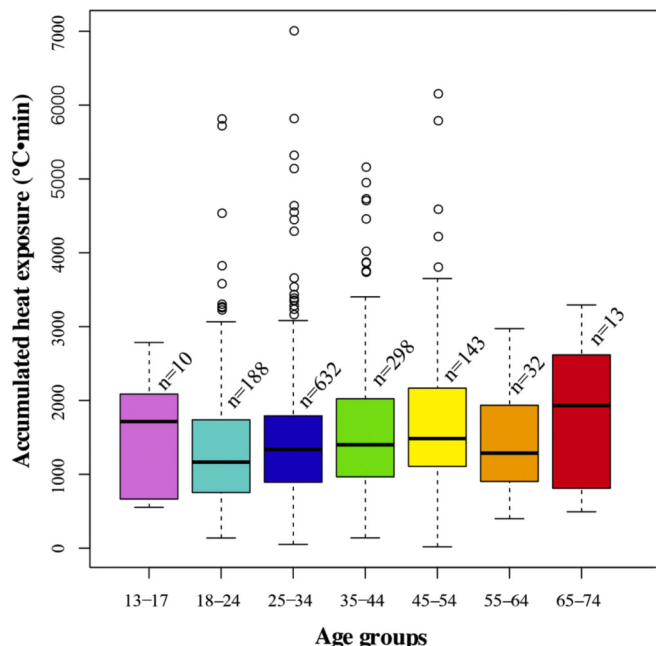


Fig. 8. The boxplot of the accumulated heat exposure ($^{\circ}\text{C}\cdot\text{min}$) among different age groups.

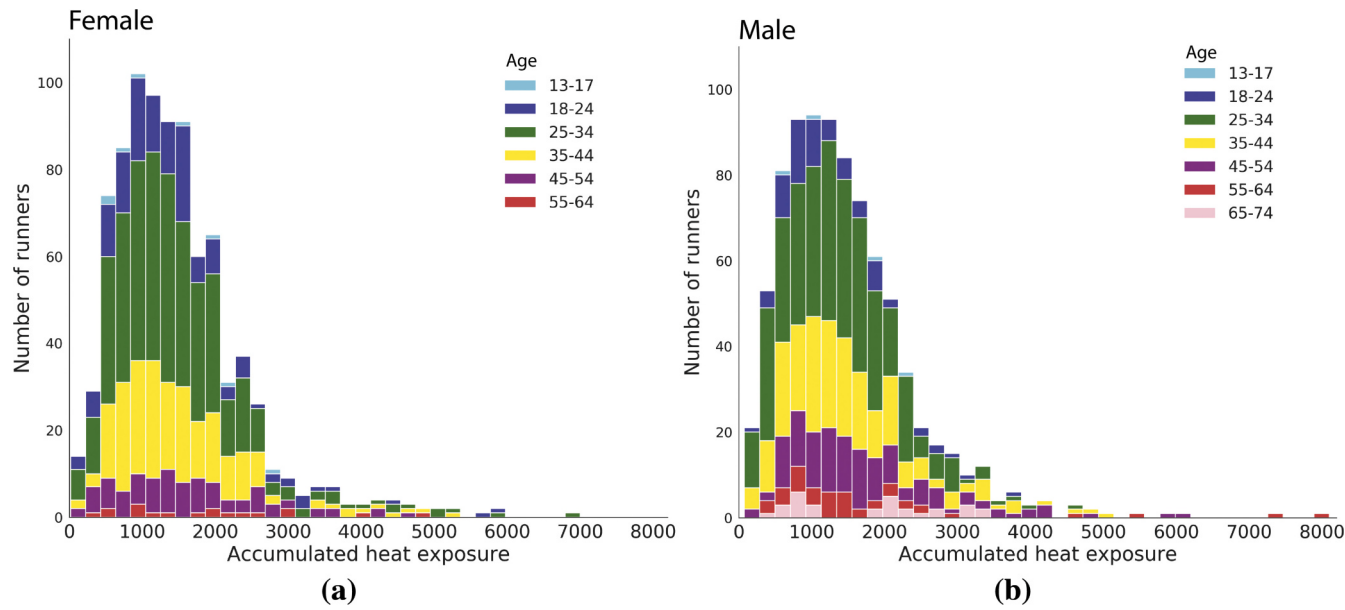


Fig. 9. The distribution of the accumulated heat exposure for female and male runners.

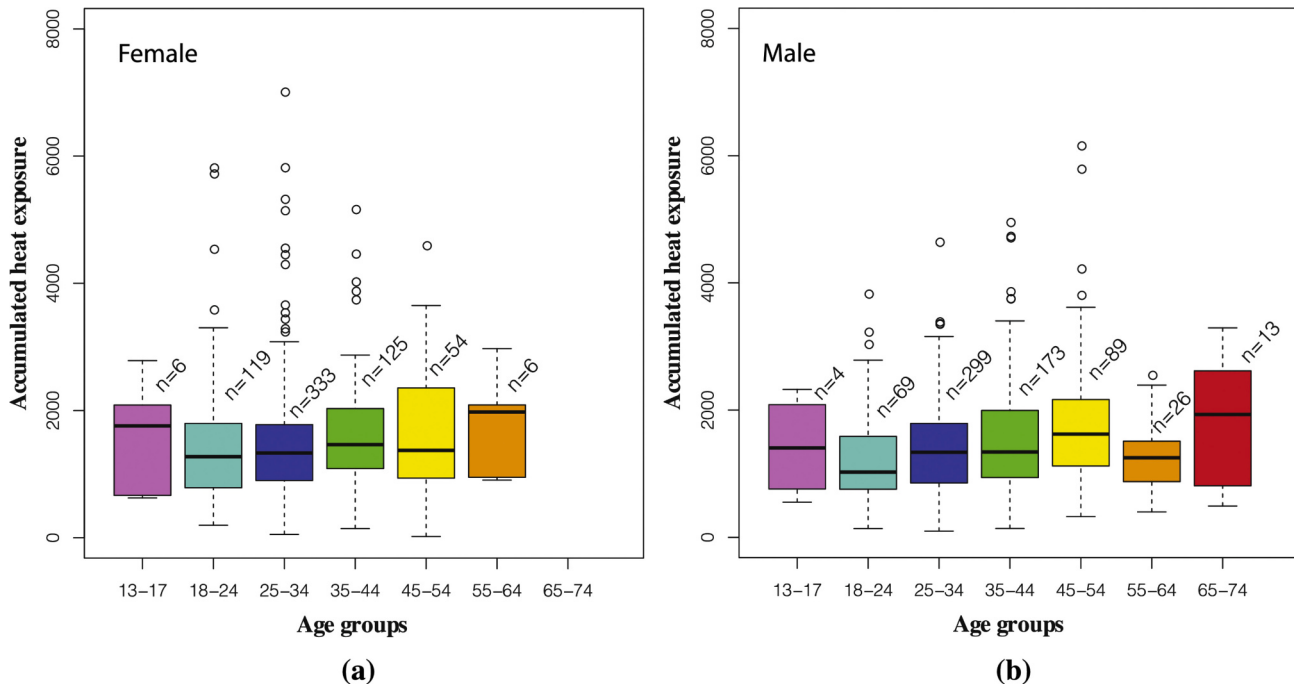


Fig. 10. The boxplots of the heat exposure for female (a) and male runners (b) of different age groups.

multispectral remotely sensed imagery and LiDAR data were used to generate the building height model and the tree canopy height model, both of which were further used as inputs for modeling the dynamic urban thermal environment with consideration of the solar and terrestrial radiation, humidity, and air temperature. The human GPS trajectories were used to indicate human travel patterns and estimate the personal accumulated heat exposure.

Different from previous coarse resolution land surface temperature derived from remotely sensed thermal imageries and the air temperature from sparsely distributed fixed-site weather stations, this study estimated the spatio-temporal distributions of the mean radiant temperature (T_{mrt}) every ten minutes with a spatial resolution of 1 m in Boston area using the SOLWEIG model. Compared with the land surface

temperature and air temperature, the T_{mrt} is the composite mean temperature of the body's radiant environment, which is more reasonable to indicate human heat exposure and indicate human body's energy balance (Huang, Cedeno-Laurent, & Spengler, 2014; Lindberg & Grimmond, 2011; Thorsson et al., 2014). The high spatio-temporal resolution T_{mrt} maps estimated in this study make it possible to indicate the temporal variations of the urban thermal environment caused by changing solar radiation and meteorological conditions in one day. In addition, the fine level T_{mrt} maps with the spatial resolution of 1 m make it possible to consider the spatial variations of thermal environment streets by streets caused by the shadow cast by buildings and tree canopies.

This study collected anonymous runner's running GPS trajectories and map-matched those trajectories to the corresponding road segments

to represent the runner's heat exposure paths. Each runner's personal heat exposure was estimated by overlaying the matched GPS trajectory coordinates on the corresponding T_{mrt} maps of the same time. This study is the first large scale study examining human personal heat exposure, which is usually related to potential heat-related health issues. Based on the proposed framework, this study also examined the different heat exposure for runners in different age-gender groups. Although most runner's heat exposure falls into the range of 1000 ($^{\circ}\text{C}\cdot\text{min}$) and 2000 ($^{\circ}\text{C}\cdot\text{min}$), runners in different age-gender groups have different heat exposure levels. Generally, there is no significant difference between female and male runners in terms of heat exposure. Runners in different age groups have different heat exposure levels, especially for female runners, as female runners in age 45–54 have significantly higher heat exposure than runners in ages of 18–24 and 25–34.

This study provides a novel framework and practice to estimate personal heat exposure with consideration of human movement along streets and high spatio-temporal resolution dynamic thermal environment. The proposed framework that combines human GPS trajectories and urban microclimate modeling based on high-resolution three-dimensional urban models makes it possible to investigate human personal heat exposure at a large spatial scale and fine temporal resolution and would benefit heat-exposure related research. The developed method is scalable based on the publicly accessible fine urban spatial data and weather data. The developed framework would also provide a general method for understanding the impact of the urban thermal environment on human well-being at a fine level. Although this study examined the runner's heat exposure, this developed framework can be directly applied to any other groups of people. The proposed framework makes it possible to examine the impacts of extreme heat events on urban residents and evaluate the potential threat of too much heat exposure in a more human-centric way, which would be helpful to reduce heat-related morbidity and mortality. In addition, the fine level spatio-temporal distribution of the T_{mrt} would also help the urban planners and decision makers to target the critical areas to mitigate the impact of extreme heat on human wellbeing and build resilience to extreme heat in future.

While the proposed framework provides a new method to estimate human heat exposure at a large scale, there are still some limitations that should be addressed in future applications. Firstly, the anonymous GPS trajectories may not be able to represent the travel patterns of the whole population of the study area. This may bring some biases to the representation of the results to a large population. The trajectories represent those people doing outdoor running, not the daily diaries, therefore future studies should think about using more objective travel diaries to better represent human daily heat exposure.

In addition, although the trajectories can indicate the human activities at the street level, the GPS trajectories and the map-matching algorithm are only able to match the trajectories to the centerlines of streets, which are different from the actual heat exposure paths. Therefore, the proposed method cannot fully indicate the internal variations inside of the street canyons. In this study, a buffer distance of 10 m was used and the average T_{mrt} was used to indicate the human exposure to minimize the uncertainty. Future studies should incorporate the sidewalk map for map-matching in order to indicate pedestrian travel patterns.

This study assumed people are running at a constant velocity and only selected the time with little cloud or clear day for the analysis. Using the weather and the time to filter out the trajectories would make the dataset cannot fully represent all runners. Because of the computational intensity, this study only simulated the weather condition and the T_{mrt} at a resolution of 10 min, and for one month. Future studies should consider using more advanced computing techniques to estimate the T_{mrt} in a longer term. Since many procedures in the SOLWEIG model is parallelizable, therefore, using GPU parallel computing would be a good option to accelerate the raster operations in SOLWEIG model and increase the efficiency.

In this study, the mean radiant temperature (T_{mrt}) was used to represent human heat exposure. Although the T_{mrt} is an objective indicator of the human body's energy balance, however, different people may have different resilience levels to heat exposure because of different personal characteristics. Future studies should also consider more personal characteristics to better indicate the potential heat exposure. Although microclimate modeling and GPS trajectory mining make it possible to scale up and investigate the human heat exposure at a large scale at any time and any location, future studies should also validate the estimated heat exposure at the personal level. Using wearable devices would be a good way to more objectively evaluate human heat exposure estimation and validate the results.

This study only empirically examined the different heat exposure levels among runners in different age-gender groups, however, the quantitative association between the heat exposure and human well-being has not been investigated. Future studies should explore the quantitative relationship between the accumulated heat exposure and human health conditions and study how this association varies among different age-gender groups. In addition, as the T_{mrt} values vary spatially across neighborhoods, future study should also explore how the socio-economic base of neighborhoods would impact human heat exposure level.

6. Conclusion

This study proposed a novel framework to investigate personal heat exposure based on anonymous GPS trajectories and urban microclimate modeling-based weather data and fine-level urban 3D models. The developed scale framework provides a new way to understand more personalized heat exposure, which would benefit heat related public health and heat-resilience building in cities. Based on the framework, this study investigated the heat exposure of anonymous runners in Boston based on the GPS trajectories and the microclimate modeling at the individual level. Results show that there is no significant difference in terms of heat exposure between the male and female runners. In different age groups, the female runners in the age group of 45–54 are significantly exposed to more heat than female runners of 18–24 and 25–34, while the heat exposure is not significantly different for males in different age groups. This study would provide us a new understanding of the different impacts of heat exposure on different genders and age groups of people for outdoor activities, which would provide new insight for investigating the impacts of outdoor heat exposure on human health and mitigating the negative impacts of heat exposure.

Authorship statement

All persons who meet authorship criteria are listed as authors, and all authors certify that they have participated sufficiently in the work to take public responsibility for the content, including participation in the concept, design, analysis, writing, or revision of the manuscript. Furthermore, each author certifies that this material or similar material has not been and will not be submitted to or published in any other publication before its appearance. The authors have conflict of interests.

Declaration of Competing Interest

None.

References

- Ali-Toudert, F., & Mayer, H. (2007). Effects of asymmetry, galleries, overhanging facades and vegetation on thermal comfort in urban street canyons. *Solar Energy*, 81(6), 742–754.
- Bailey, E., Fuhrmann, C., Runkle, J., Stevens, S., Brown, M., & Sugg, M. (2020). Wearable sensors for personal temperature exposure assessments: A comparative study. *Environmental Research*, 180, 108858.

- Basu, R., & Samet, J. M. (2002). An exposure assessment study of ambient heat exposure in an elderly population in Baltimore, Maryland. *Environmental Health Perspectives*, 110(12), 1219–1224.
- Bernhard, M. C., Kent, S. T., Sloan, M. E., Evans, M. B., McClure, L. A., & Gohlike, J. M. (2015). Measuring personal heat exposure in an urban and rural environment. *Environmental Research*, 137, 410–418.
- Borden, K. A., & Cutter, S. L. (2008). Spatial patterns of natural hazards mortality in the United States. *International Journal of Health Geographics*, 7(1), 64.
- Gasparotto, T., & Nesselser, C. (2020). Diverse effects of thermal conditions on performance of marathon runners. *Frontiers in Psychology*, 11, 1438.
- Gasparrini, A., Guo, Y., Hashizume, M., Lavigne, E., Zanobetti, A., Schwartz, J., ... Leone, M. (2015). Mortality risk attributable to high and low ambient temperature: A multicountry observational study. *The Lancet*, 386(9991), 369–375.
- Hajat, S., O'Connor, M., & Kosatsky, T. (2010). Health effects of hot weather: From awareness of risk factors to effective health protection. *The Lancet*, 375(9717), 856–863.
- Harlan, S. L., Declet-Barreto, J. H., Stefanov, W. L., & Petitti, D. B. (2013). Neighborhood effects on heat deaths: Social and environmental predictors of vulnerability in Maricopa County, Arizona. *Environmental Health Perspectives*, 121(2), 197–204.
- Hass, A. L., & Ellis, K. N. (2019). Using wearable sensors to assess how a heatwave affects individual heat exposure, perceptions, and adaption methods. *International Journal of Biometeorology*, 63(12), 1585–1595.
- Ho, H. C., & Wong, M. S. (2019). Urban environmental influences on the temperature–mortality relationship associated mental disorders and cardiopulmonary diseases during normal summer days in a subtropical city. *Environmental Science and Pollution Research*, 26(23), 24272–24285.
- Honjo, T., Seo, Y., Yamasaki, Y., Tsunematsu, N., Yokoyama, H., Yamato, H., & Mikami, T. (2018). Thermal comfort along the marathon course of the 2020 Tokyo Olympics. *International Journal of Biometeorology*, 62(8), 1407–1419.
- Huang, J., Cedeno-Laurent, J. G., & Spengler, J. D. (2014). CityComfort+: A simulation-based method for predicting mean radiant temperature in dense urban areas. *Building and Environment*, 80, 84–95.
- Jenerette, G. D., Harlan, S. L., Buyantuev, A., Stefanov, W. L., Declet-Barreto, J., Ruddell, B. L., ... Li, X. (2016). Micro-scale urban surface temperatures are related to land-cover features and residential heat related health impacts in Phoenix, AZ USA. *Landscape Ecology*, 31(4), 745–760.
- Kovats, R. S., & Hajat, S. (2008). Heat stress and public health: A critical review. *Annual Review of Public Health*, 29, 41–55.
- Kuras, E. R., Richardson, M. B., Calkins, M. M., Ebi, K. L., Hess, J. J., Kintziger, K. W., ... Hondula, D. M. (2017). Opportunities and challenges for personal heat exposure research. *Environmental Health Perspectives*, 125(8), Article 085001.
- Li, X. (2021). Investigating the spatial distribution of resident's outdoor heat exposure across neighborhoods of Philadelphia, Pennsylvania using urban microclimate modeling. *Sustainable Cities and Society*, Article 103066.
- Li, X., & Ratti, C. (2019). Mapping the spatio-temporal distribution of solar radiation within street canyons of Boston using Google Street View panoramas and building height model. *Landscape and Urban Planning*, 191, 103387.
- Li, X., Santi, P., Courtney, T. K., Verma, S. K., & Ratti, C. (2018). Investigating the association between streetscapes and human walking activities using Google Street View and human trajectory data. *Transactions in GIS*, 22(4), 1029–1044.
- Lindberg, F., & Grimmond, C. S. B. (2011). The influence of vegetation and building morphology on shadow patterns and mean radiant temperatures in urban areas: Model development and evaluation. *Theoretical and Applied Climatology*, 105(3–4), 311–323.
- Lindberg, F., Holmer, B., & Thorsson, S. (2008). SOLWEIG 1.0—Modelling spatial variations of 3D radiant fluxes and mean radiant temperature in complex urban settings. *International Journal of Biometeorology*, 52(7), 697–713.
- Lindberg, F., Holmer, B., Thorsson, S., & Rayner, D. (2014). Characteristics of the mean radiant temperature in high latitude cities—Implications for sensitive climate planning applications. *International Journal of Biometeorology*, 58(5), 613–627.
- Malleson, N., Vanký, A., Hashemian, B., Santi, P., Verma, S. K., Courtney, T. K., & Ratti, C. (2018). The characteristics of asymmetric pedestrian behavior: A preliminary study using passive smartphone location data. *Transactions in GIS*, 22(2), 616–634.
- Mayer, H., & Höpke, P. (1987). Thermal comfort of man in different urban environments. *Theoretical and Applied Climatology*, 38(1), 43–49.
- Middel, A., Lukasczyk, J., & Maciejewski, R. (2017). Sky view factors from synthetic fisheye photos for thermal comfort routing—A case study in Phoenix, Arizona. *Urban Planning*, 2(1), 19–30.
- Milà, C., Curto, A., Dimitrova, A., Sreekanth, V., Kinra, S., Marshall, J. D., & Tonne, C. (2020). Identifying predictors of personal exposure to air temperature in peri-urban India. *Science of the Total Environment*, 707, 136114.
- Muller, C. L., Chapman, L., Johnston, S., Kidd, C., Illingworth, S., Foody, G., ... Leigh, R. R. (2015). Crowdsourcing for climate and atmospheric sciences: Current status and future potential. *International Journal of Climatology*, 35(11), 3185–3203.
- National Weather Service. (2018). 78-year list of severe weather fatalities. http://www.nws.noaa.gov/om/hazstats/resources/weather_fatalities.pdf.
- Nazarian, N., Liu, S., Kohler, M., Lee, J. K., Miller, C., Chow, W. T., ... Norford, L. K. (2021). Project Coolbit: Can your watch predict heat stress and thermal comfort sensation? *Environmental Research Letters*, 16(3), Article 034031.
- Newson, P., & Krumm, J. (2009, November). Hidden Markov map matching through noise and sparseness. In *Proceedings of the 17th ACM SIGSPATIAL international conference on advances in geographic information systems* (pp. 336–343).
- Noelke, C., McGovern, M., Corsi, D. J., Jimenez, M. P., Stern, A., Wing, I. S., & Berkman, L. (2016). Increasing ambient temperature reduces emotional well-being. *Environmental Research*, 151, 124–129.
- Parsons, K. (2003). *Human thermal environments, the effects of hot, moderate and cold temperatures on human health, comfort and performance* (2nd ed.). New York: CRC Press.
- Pearce, H. (2017). Staying cool in the compact city: Vacant land and urban heating in Philadelphia, Pennsylvania. *Applied Geography*, 79, 84–92.
- Reidmiller, D. R., Avery, C. W., Easterling, D. R., Kunkel, K. E., Lewis, K. L. M., Maycock, T. K., & Stewart, B. C. (Eds.). (2018). Vol. II. *Impacts, risks, and adaptation in the United States: Fourth national climate assessment*. Global Change Research Program. <https://doi.org/10.7930/nca4.2018>.
- Stone, B., Hess, J. J., & Frumkin, H. (2010). Urban form and extreme heat events: Are sprawling cities more vulnerable to climate change than compact cities? *Environmental Health Perspectives*, 118(10), 1425–1428.
- Stone, B., Jr., Lanza, K., Mallen, E., Vargo, J., & Russell, A. (2019). Urban heat management in Louisville, Kentucky: A framework for climate adaptation planning. *Journal of Planning Education and Research* (0739456X19879214).
- Thorsson, S., Rocklöv, J., Konarska, J., Lindberg, F., Holmer, B., Dousset, B., & Rayner, D. (2014). Mean radiant temperature—A predictor of heat related mortality. *Urban Climate*, 10, 332–345.
- Vanos, J. K., Kosaka, E., Iida, A., Yokohari, M., Middel, A., Scott-Fleming, I., & Brown, R. D. (2019). Planning for spectator thermal comfort and health in the face of extreme heat: The Tokyo 2020 Olympic marathons. *Science of the Total Environment*, 657, 904–917.
- Venter, Z. S., Krog, N. H., & Barton, D. N. (2020). Linking green infrastructure to urban heat and human health risk mitigation in Oslo, Norway. *Science of the Total Environment*, 709, 136193.
- Wang, C., Li, Y., Myint, S. W., Zhao, Q., & Wentz, E. A. (2019). Impacts of spatial clustering of urban land cover on land surface temperature across Köppen climate zones in the contiguous United States. *Landscape and Urban Planning*, 192, 103668.
- Wang, C., Zhang, Z., Zhou, M., Wang, P., Yin, P., Ye, W., & Zhang, L. (2018). Different response of human mortality to extreme temperatures (MoET) between rural and urban areas: A multi-scale study across China. *Health & Place*, 50, 119–129.
- Zhang, F., de Dear, R., & Hancock, P. (2019). Effects of moderate thermal environments on cognitive performance: A multidisciplinary review. *Applied Energy*, 236, 760–777.